

# Mull-Tokens: Modality-Agnostic Latent Thinking

Arijit Ray<sup>1,4</sup> Ahmed Abdelkader<sup>1</sup> Chengzhi Mao<sup>1</sup> Bryan A. Plummer<sup>4</sup> Kate Saenko<sup>4</sup>  
 Ranjay Krishna<sup>2</sup> Leonidas Guibas<sup>1,3</sup> Wen-Sheng Chu<sup>1</sup>

<sup>1</sup>Google <sup>2</sup>University of Washington <sup>3</sup>Stanford University <sup>4</sup>Boston University

[https://arijitray.com/multimodal\\_thinking/](https://arijitray.com/multimodal_thinking/)

## Abstract

*Reasoning goes beyond language; the real world requires reasoning about space, time, affordances, and much more that words alone cannot convey. Existing multimodal models exploring the potential of reasoning with images are brittle and do not scale. They rely on calling specialist tools, costly generation of images, or handcrafted reasoning data to switch between text and image thoughts. Instead, we offer a simpler alternative – Mull-Tokens – modality-agnostic latent tokens pre-trained to hold intermediate information in either image or text modalities to let the model think free-form towards the correct answer. We investigate best practices to train Mull-Tokens inspired by latent reasoning frameworks. We first train Mull-Tokens using supervision from interleaved text-image traces, and then fine-tune without any supervision by only using the final answers. Across four challenging spatial reasoning benchmarks involving tasks such as solving puzzles and taking different perspectives, we demonstrate that Mull-Tokens improve upon several baselines utilizing text-only reasoning or interleaved image-text reasoning, achieving a +3% average improvement and up to +16% on a puzzle solving reasoning-heavy split compared to our strongest baseline. Adding to conversations around challenges in grounding textual and visual reasoning, Mull-Tokens offers a simple solution to abstractly think in multiple modalities.*

## 1. Introduction

Real-world visual tasks [57, 58] require a synchrony of perception and reasoning [26]. For example, when solving visual puzzles and IQ tests, people imagine patterns and manipulate visual maps to solve the problem [42]. Such reasoning—often bundled up as visual/spatial reasoning [48]—is difficult for humans and machines alike [66]. It requires reasoning in space [29], in 3D [5, 32], and often in time [6, 66]. While textual Chain-of-Thought (CoT) [61]

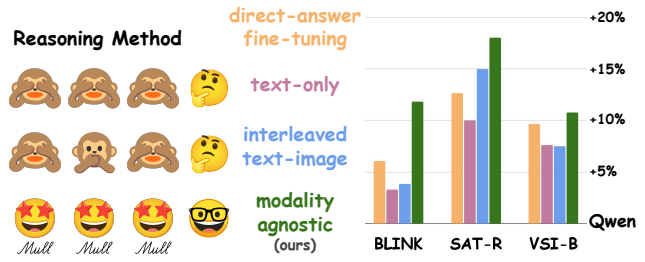


Figure 1. Compared to existing approaches for reasoning in text or interleaving image and text, we offer a simpler alternative – modality-agnostic thinking in the vision-language space using Mull-Tokens to answer visual queries.

has advanced verbal logical reasoning for language models, it falls short on visual reasoning: models still falter when problems demand more than verbal image descriptions [2, 38, 59]. Mastering *vision-centric* logical reasoning remains an open challenge.

To advance visual reasoning, researchers have explored “think-and-sketch” strategies [26, 44] using interleaved visual thoughts, but with conflicting results [32]. Tool-augmented designs rely on external visual modules [41] such as cropping tools [44] or specialized sketching models [26, 77] – making the reasoning indirect and often brittle [23]. Unified models [8, 13, 53] offer a more integrated alternative by generating intermediate images but are expensive to train. The latest visual reasoning models instead use image thoughts, either as explicit visual tokens [5] or dense continuous embeddings [68]. However, they require bespoke task-specific training data and hence, do not offer a general recipe for visual reasoning. For instance, we find that naively adding *modality-specific* reasoning supervision can sometimes hurt: supervising a model to interleave textual thoughts and visual latents actually reduced performance on a visual puzzle solving task compared to reasoning in text. Hence, an effective strategy to use the growing availability of multimodal CoT traces [7, 30] remains elusive.

To address this gap, we present *Null-Tokens*: *modality-agnostic* latent tokens that function as a multimodal scratchpad for the model’s internal reasoning, capable of representing *both visual or textual information* as needed. During inference, we append these special tokens to the input question, prompting the model to utilize those modality-agnostic slots for arbitrary intermediate computations (spatial mappings, depth predictions, verbal manipulations, etc.) towards the answer, without the need for explicit decoding into text or images.

Inspired by recent latent reasoning frameworks [22, 49, 68, 69], we develop a two-stage curriculum for training a model to use *Null-Tokens* effectively. The first stage trains the model using multimodal reasoning traces where each *Null-Token* is *anchored* to a relevant textual or visual concept [30]. For example, one token might learn to encode a visual object layout or a textual symbolic mapping if those are useful for the task at hand. The second stage relaxes the supervision on *Null-Tokens* and fine-tunes the model using only the final answer. This stage gives the model an opportunity for optimizing its latent trajectories freely, so as to maximize end-task performance. *Null-Tokens* augment a model’s vocabulary, similar to special tokens (e.g. `<plan>` or `<pause>`) used in reasoning models [5, 22]. Finally, we follow by a third refinement stage leveraging the latest reinforcement learning (RL) techniques [24] to reward the latent chain of “thinking.”

We fine-tune a Multimodal Language Model (MLM), Qwen2.5-VL (7B) [3], with *Null-Tokens* as described above. We then evaluate the resulting model on a wide range of visual reasoning benchmarks covering both images and videos. In particular, we test on spatial reasoning problems such as visual puzzles and IQ-tests from BLINK [19], VSI-Bench (video spatial reasoning), SAT [48] (action and motion-based spatial relationship reasoning), and ERQA [55] (robotics action consequences and trajectories), offering a thorough evaluation of *Null-Tokens*’ capabilities.

Across all benchmarks, our *Null-Tokens* significantly improve the model’s reasoning accuracy compared to both standard answer-only fine-tuning, textual reasoning, and a recent approach interleaving explicit text reasoning with image latents [68]. On average, *Null-Tokens* achieve a +3% absolute accuracy gain over our strongest baseline, which is surprisingly obtained by fine-tuning the base model directly on answers without reasoning. The benefits of *Null-Tokens* are even larger on the most reasoning-intensive tasks, improving +16% on a visual puzzle split.

These results echo the gains reported by prior works when introducing learned visual tokens [5], but we emphasize that our approach requires far fewer and modality-agnostic tokens, without task-specific data for training. Only 10–40 *Null-Tokens* are sufficient to yield the above

improvements. This is a drastic reduction in inference overhead compared to generating hundreds of word tokens in a typical text CoT rationale, or hundreds of visual tokens to represent an image, reminiscent of findings that shorter reasoning traces can be just as effective [52].

In summary, our contributions are:

1. An effective thinking paradigm utilizing discrete modality-agnostic *Null-Tokens*, improving upon the base model by 9% with up to 16% on reasoning-heavy splits, while being faster than existing works that produce verbose thoughts [17] or generate explicit images as thoughts [5].
2. Improving by 4% over the latest prior approach of interleaving visual thoughts with text, based on explicit switching between the two modalities [68], establishing the superiority of our modality-agnostic approach.
3. Extensive ablations identifying the best design choices for integrating visual thoughts with text reasoning - establishing the necessity of multimodal (joint visual and textual) data for training *Null-Tokens* - where simply using latent tokens with text only or extra compute without multimodal anchoring doesn’t suffice.

Adjacent to recent work that suggest MLMs overlook the rich information already present in the visual encoders [18, 34, 35, 45], *Null-Tokens* offers a simple approach to help models to use and manipulate visual signals for improved multimodal reasoning performance.

## 2. Related Work

The primary theme of our work concerns the incorporation of multi-modal latents to enhance the visual and spatial reasoning capabilities [10, 48, 66] of MLMs [3, 75].

**Visual Reasoning.** Building upon powerful perception in vision-language models [1, 37], there has been great interest in improving reasoning over both modalities [27, 76]. Inspired by the success of textual CoT reasoning in language models [16, 60], recent works have looked into using similar techniques for visual questions [17, 40]. Due to limitations of textual reasoning for visual tasks [23, 40], many works now reason using visual thoughts as well-but rely on expensive unified models [39, 51, 53, 63–65, 72] to explicitly generate images [14, 23, 30, 74], or latents [5, 11, 31, 68, 68, 70, 73], or external tools that may be brittle [26, 44]. We aim to incorporate latents as simpler direct and less expensive alternative without needing bespoke data [68]. While fixing problems with textual reasoning using text alone is a valid avenue for exploration [17, 33, 40], we offer a simpler and faster alternative of appending a few modality agnostic thinking tokens. Within visual reasoning, there is recently a special emphasis on spatial reasoning [29, 36, 55, 56, 66, 75] with an increased variety of spatial annotations [12, 48], benchmarks [19, 54, 55, 66], and data curation [17, 47, 56, 67].

Our work contributes to training paradigms for improving spatial reasoning [5, 6, 12, 15, 43, 48, 67].

**Latent Reasoning.** Our thinking tokens are heavily inspired by latent reasoning techniques in language models [22, 25, 49]. A closely related theme is test-time scaling, allocating more compute at inference time before producing an answer [22, 28, 50]. While some approaches adopt recurrent models over continuous tokens [20, 25, 78], they break standard parallel processing and accumulate errors [25, 68]. Hence, we adopt discrete think tokens with a rich internal recurrence achieving substantial gains.

### 3. Approach

Our primary objective is to improve the visual reasoning performance of multimodal language models [1, 37]. Formally, the model with parameters  $\theta$  implements a conditional distribution  $p_\theta(y|x^{\text{img}}, x^{\text{txt}})$ , where  $x^{\text{img}}$  and  $x^{\text{txt}}$  denote the visual and textual inputs, and  $y$  is the target answer sequence.

Textual Chain-of-Thought (CoT) augments this input-output mapping with intermediate textual tokens  $c_{1:T}^{\text{text}}$  effective for verbal reasoning, but often detrimental for visual tasks [66] due to problems such as drifting from visual inputs [40]. Recent approaches therefore supervise models to “think with images,” e.g., by generating intermediate images or visual sketches  $c_{1:T}^{\text{img}}$  during reasoning [5, 23, 26]. However, these methods typically require (i) bespoke multimodal reasoning datasets  $\mathcal{D}_{CoT}$  with aligned text–image chains, or (ii) expensive generation of subgoal images that are hard to generalize beyond the specific training domains.

We instead introduce a simpler, modality-agnostic mechanism, *Mull-Tokens*, implemented as a fixed-length sequence of special latent tokens  $z_{1:K} = (<\text{Mull}>_1, \dots, <\text{Mull}>_K)$ , which can carry both image-conditioned and text-conditioned information. During training and inference, the model can use these tokens purely as *internal compute* to improve visual reasoning, without being constrained to produce textual or image outputs at the intermediate steps.

At a high level, we replace explicit CoT supervision on intermediate text/images with supervision on the *function* of the latent chain: the model is trained so that using  $z_{1:K}$  improves  $p_\theta(y | x^{\text{img}}, x^{\text{txt}})$ , while the internal semantics of  $z_{1:K}$  are free to adapt. Below, we formalize our two-stage latent reasoning framework and a third RL refinement stage.

#### Modality-agnostic *Mull-Tokens*

Inspired by latent reasoning approaches in NLP [22], our training is decomposed into three stages (Figure 2): (1) *warm-up* the *Mull-Tokens* tokens to align with explicit multimodal reasoning steps; (2) *relax* supervision to only the final answer, allowing the model to optimize the latent chain internally; and (3) *refine* the causal usefulness of the

latents via GRPO. Our base backbone is Qwen2.5-VL [3], which provides a text decoder and a frozen image encoder.

#### Stage 1: Warm-up the *Mull-Tokens* tokens

Let  $\mathcal{D}_{CoT}$  be a dataset (see Figure 2 (left)) of multimodal CoT trajectories. Each training example consists of an input  $(x^{\text{img}}, x^{\text{txt}})$ , a reasoning trace

$$c_{1:T} = (c_1, \dots, c_T), \quad c_t \in \mathcal{V}^{\text{txt}} \cup \mathcal{V}^{\text{img}},$$

and a final answer sequence  $y_{1:L}$ . Here,  $\mathcal{V}^{\text{txt}}$  is the text vocabulary and  $\mathcal{V}^{\text{img}}$  denotes “pseudo-tokens” corresponding to subgoal images (e.g., the jigsaw configuration after inserting a candidate piece).

We construct an interleaved training sequence

$$s = (q_{1:M}, z_1, \tilde{c}_1, z_2, \tilde{c}_2, \dots, z_T, \tilde{c}_T, y_{1:L}),$$

where  $q_{1:M}$  encodes the question and context,  $\tilde{c}_t$  is the textual substep or an image placeholder for  $c_t$ , and  $z_t = <\text{Mull}>_t$  is the  $t$ -th latent token. The transformer is trained in an auto-regressive manner over  $s$ .

Let  $h_t^{\text{Mull}} \in \mathbb{R}^d$  denote the hidden state at the position of  $z_t$  produced by the transformer. We apply *two* kinds of supervision:

- If  $c_t \in \mathcal{V}^{\text{txt}}$  (next step is a word token), we warp  $h_t^{\text{Mull}}$  through the language model head to predict  $p_\theta(c_t | s_{<t})$  and minimize the cross-entropy  $\mathcal{L}_t^{\text{text}} = -\log p_\theta(c_t | s_{<t})$ .
- If  $c_t \in \mathcal{V}^{\text{img}}$  is (a subgoal image  $I_t \in \mathbb{R}^{H \times W \times 3}$ ), we encode it using the frozen Qwen2.5-VL image encoder  $g_\phi: v_t = g_\phi(I_t) \in \mathbb{R}^d$ . We then supervise  $h_t^{\text{Mull}}$  via cosine similarity:  $\mathcal{L}_t^{\text{img}} = 1 - \cos(\hat{h}_t, \hat{v}_t)$

The full Stage-1 objective for a sequence  $s$  is

$$\mathcal{L}_{\text{stage1}} = \sum_{i \in \mathcal{I}_{\text{AR}}} \mathcal{L}_i^{\text{AR}} + \lambda_{\text{text}} \sum_{t \in \mathcal{T}_{\text{text}}} \mathcal{L}_t^{\text{text}} + \lambda_{\text{img}} \sum_{t \in \mathcal{T}_{\text{img}}} \mathcal{L}_t^{\text{img}},$$

where  $\mathcal{I}_{\text{AR}}$  indexes standard tokens (question and answer) with conventional next-token cross-entropy  $\mathcal{L}_i^{\text{AR}}$ , and  $\mathcal{T}_{\text{text}} / \mathcal{T}_{\text{img}}$  index  $<\text{Mull}>$  positions followed by text or image steps, respectively.

This setup naturally extends to other modalities (e.g., 3D or trajectory representations) by changing the embedding function  $g_\phi$  and similarity loss; we leave this extension to future work in the absence of such multimodal CoT data.

#### Stage 2: *Mull-Tokens* Relaxed training

After warm-up, we transition to a relaxed training stage where the latent tokens are no longer explicitly supervised on the next reasoning step. Let  $s' = (q_{1:M}, z_{1:K}, y_{1:L})$  denote the sequence where  $z_{1:K}$  is inserted after the question, but the intermediate CoT steps are no longer present.

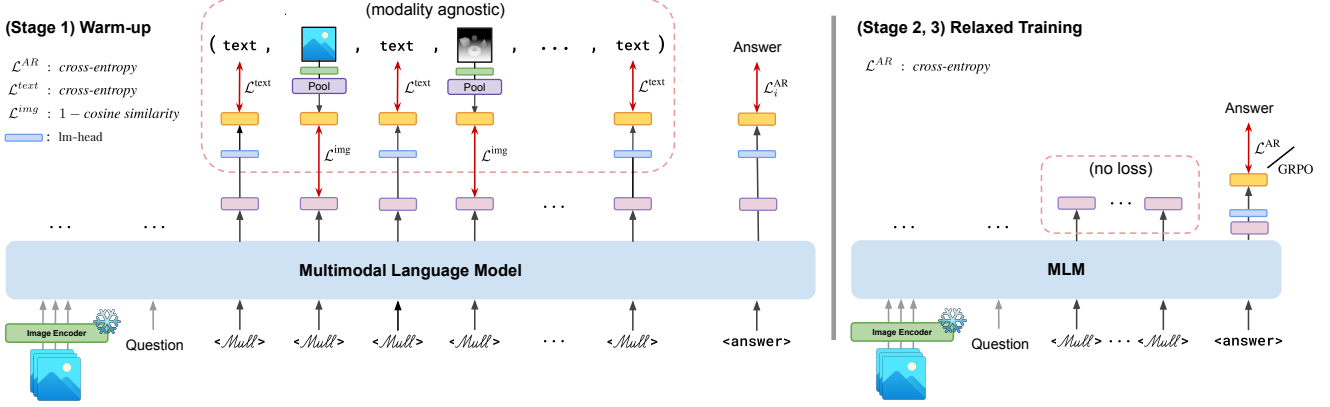


Figure 2. Our *Mull-Tokens* training involves two stages inspired by approaches in latent reasoning. We first pre-train/warm-up our *Mull-Tokens* to hold both image and text modalities depending on the context image/video and query. Next, the model free-form optimizes these *Mull-Tokens* to achieve the final correct answer. We see that pre-training the *Mull-Tokens* with to hold both image and text reasoning traces is key, as opposed to using them simply as extra compute without such pretraining or using text alone.

We now optimize only the answer likelihood and drop all losses on  $z_{1:K}$ .

$$\mathcal{L}_{\text{stage2}} = - \sum_{\ell=1}^L \log p_{\theta}(y_{\ell} | s'_{<\ell}),$$

This relaxation is critical: the model is not forced to mimic the potentially suboptimal supervised CoT scaffolding from Stage 1. Instead,  $z_{1:K}$  becomes an internal scratchpad whose semantics are determined solely by how much they help minimize  $\mathcal{L}_{\text{stage2}}$  on the final answer.

A key design choice is the form of recurrence used for multimodal latents. Let  $z_t^{\text{cont}} \in \mathbb{R}^d$  denote continuous recurrent latents as in [25, 68]. These approaches explicitly iterate over  $t$ :  $z_{t+1}^{\text{cont}} = f_{\theta}(z_t^{\text{cont}}, x)$ , requiring sequential updates both at training and inference time, and leading to: (i) *inefficiency*, since they break standard parallel token processing in transformers; and (ii) *instability*, since errors accumulate over long chains, as empirically noted in [25, 68].

Therefore, we adopt discrete token latents as in [5, 22]. We allocate a fixed number  $K$  of  $\langle \text{Mull} \rangle$  tokens in the sequence. Let  $H^{\text{Mull}} = (h_1^{\text{Mull}}, \dots, h_K^{\text{Mull}})$  denote their hidden states after the transformer layers; these states are jointly computed via standard self-attention, and then attended to by the answer tokens  $y_{1:L}$ . We ablate  $K$  as a hyperparameter in our experiments. This design is compatible with transformer parallelism, while still allowing rich internal recurrence through self-attention over  $z_{1:K}$ .

### Stage 3: RL Refinement with GRPO

Although Stage 2 encourages the model to *use Mull-Tokens* to reduce answer loss, it does not enforce that the latent chain is *causally* responsible for the final prediction. In principle, the model could learn a shortcut mapping from  $(x^{\text{img}}, x^{\text{txt}})$  directly to  $y$  and ignore  $z_{1:K}$ , e.g., by placing

most of the computation in the final layers conditioned only weakly on the  $\langle \text{Mull} \rangle$  states.

To explicitly reward latent chains that causally contribute to the correct answer, we introduce a third stage based using GRPO [24], following recent text-based reasoning frameworks [9, 17]. While we can perform this GRPO refinement right after Stage 1, we found that first doing stage 2 is critical. The model is not optimized to effectively use the *Mull-Tokens* after Stage 1, and the sparse rewards from just the final answer is not enough to optimize the performance.

Let  $\pi_{\theta}(y_{1:L}, z_{1:K} | x)$  denote the policy induced by the MLM, where  $x = (x^{\text{img}}, x^{\text{txt}})$ , and  $z_{1:K}$  are sampled internal latents (or deterministically generated but treated as part of the trajectory). For each training instance with ground truth answer  $y^*$ , we define a reward

$$r(y_{1:L}, y^*) = \begin{cases} 1, & \text{if } y_{1:L} \text{ discrete answers} \\ \text{score}(y_{1:L}, y^*) & \text{if numeric / continuous,} \end{cases}$$

where score is a graded similarity, e.g., based on normalized absolute error; the exact form detailed in the supplementary.

In practice, we follow the standard GRPO update that effectively shapes the gradients to emphasize reward-improving trajectories. Because our *Mull-Tokens* are a fixed discrete prefix of length  $K$ , and the first answer token  $y_1$  is sampled from the final *Mull* state (*i.e.*, its hidden representation  $h_K^{\text{Mull}}$  under self-attention), the gradient signal for  $r$  flows back primarily through  $h_K^{\text{Mull}}$  and, via self-attention, through the entire latent chain  $h_{1:K}^{\text{Mull}}$ . Thus, GRPO refines the latent trajectories  $(h_1^{\text{Mull}}, \dots, h_K^{\text{Mull}})$  that *causally* lead to correct answers, rather than merely co-occurring with them.

## 4. Experiments

We evaluate and ablate *Mull-Tokens* on four recent challenging visual reasoning benchmarks to assess: i) improve-

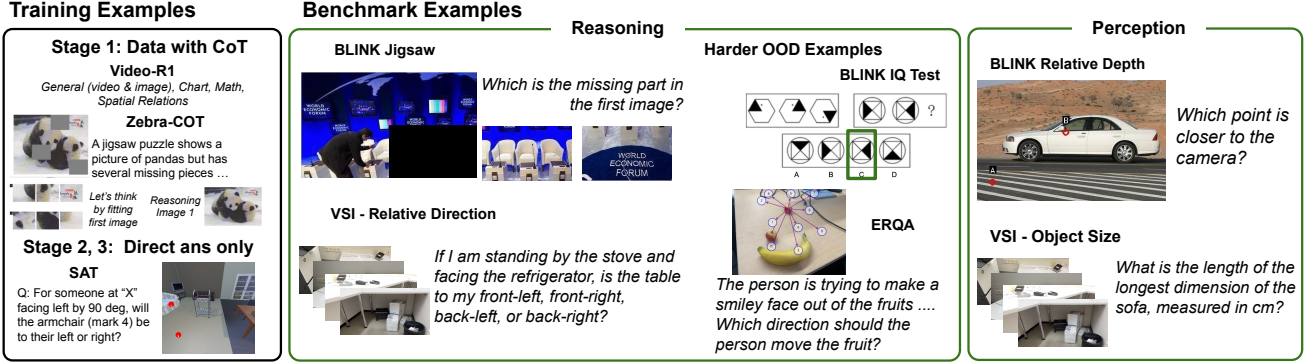


Figure 3. Examples of training and our benchmark data. We test on diverse reasoning benchmarks, which includes hard examples that do not have the reasoning outlined in the training sets. Our training consists of two types of data- general video QA's with text reasoning, data of interleaved image text reasoning, and data with only the final answer.

ments compared to existing visual reasoning paradigms of reasoning in text or interleaving visual thoughts, ii) how important multimodal information in *Mull-Tokens* is for performance gains - showing *multimodal* thinking compute is crucial for performance compared to text-only or extra compute without such anchoring, and iii) scaling behavior with latent tokens and recurrence design choices when using *Mull-Tokens* - showing discrete tokens [22] deliver better performance and speed continuous embeddings used in recent work [25, 68].

#### 4.1. Experimental setup

**Base model.** We choose a powerful open-source multimodal language model, Qwen2.5-VL (7B) model [3] as our base since it is also used in existing visual reasoning works [17, 40, 68]. All our ablations and baselines are trained using 8 H100 (80GB) GPUs using DeepSpeed [46].

**Evaluation benchmarks.** To test performance, we evaluate the answer accuracy on spatial questions for images and videos across four recent benchmarks that test a variety of capabilities such as understanding camera motion, taking perspectives, and solving visual puzzles and IQ tests. Below we highlight the specific benchmarks we use (also displayed in Figure 3):

**BLINK** [19] We focus on the spatial splits in BLINK - multi-view reasoning dealing with camera movements between two images (MV), relative depths (RelDep), spatial relations (SpRel), jigsaw puzzles (Jig) and IQ Tests (IQT). We group multi-view reasoning, jigsaw puzzles and IQ tests as *reasoning* splits since they require comparing/manipulating visual elements as report a reasoning average (*Reas* in the Tables) along with the overall average.

**SAT-Real (SAT-R)** [48] This includes questions that require reasoning about actions and motions based on a single image or a sequence of images.

**VSI-Bench (VSI-B)** [66] This is a video benchmark with

walkthroughs of indoor scenes and questions about object sizes, distances, relations from other perspectives, and optimal routes. We group relative direction, relative distance, and route planning into the reasoning splits. These splits ask questions about relationships from a different perspective or planning routes, that requires manipulating visual and symbolic elements. We report this subset average as *Reas* under the VSI-Bench column in the tables.

**ERQA** [55] This is an embodied robotics question answering dataset that focuses questions about object trajectories to complete goals, consequences of actions on images, and estimating the state of completion of tasks based on a single image input.

We would like to note that some benchmark numbers, especially on videos may differ from existing work due to number of frames used and the answer fuzzy matching logic. We modify the widely-used framework lmms-eval [71] for our evaluations. We maintain the same frame count, answer matching logic, and prompt format across all our baselines and ablations to avoid such confounding factors in performance differences.

**Training datasets.** We use three datasets: Video-R1, Zebra-CoT, and SAT as shown in Figure 3. Exact data mixtures for each of stages are in the appendix.

**Video-R1** [17] is a general video reasoning dataset with reasoning traces containing 160K examples. It contains videos and images with questions spanning multiple topics like chart understanding, spatial reasoning, and perception tasks. We use this dataset primarily during *Stage-1*, where we train the *Mull-Tokens* tokens with CoT traces.

**Zebra-CoT** [30] is a recent image-text interleaved CoT dataset with reasoning traces that include both text and sub-goal images as reasoning traces towards the answer for a range of visual and spatial tasks such as playing chess, solving puzzles, and counting. We use this dataset primarily during *Stage 1* to train *Mull-Tokens* for intermediate rea-

Table 1. *Null-Tokens* (row f, g) improve over direct answer finetuning (row b), and existing methods for visual reasoning tasks using text-only reasoning (row c, d) [9, 17], or text-image interleaving (row e) [68]. Data splits are described in Section 4.1.

Model	BLINK							SAT-R		VSI		ERQA	Avg(All)
	MV	RelDep	SpRel	Jig	IQT	Avg	Reas	Avg	Reas	Avg	Reas		
a. Qwen2.5-VL (7B)	39.00	61.29	<b>92.38</b>	58.66	25.33	55.33	41.00	59.00	23.96	22.96	<b>38.91</b>	44.30	
b. + DirAns FT	57.14	<b>87.09</b>	74.12	58.66	30.00	61.40	48.60	71.66	32.40	30.65	38.00	50.87	
c. + TextCoT FT	53.38	74.19	67.83	69.30	25.33	58.01	49.34	68.33	30.47	31.04	38.78	48.90	
$\Delta$ (vs. DirAns)	-3.76	-12.90	-6.29	+10.64	-4.67	-3.39	+0.74	-3.33	-1.93	+0.39	+0.78	-1.97	
d. + GRPO	54.88	71.77	69.23	72.00	25.33	58.64	50.74	69.00	30.34	30.15	36.00	48.50	
$\Delta$ (vs. DirAns)	-2.26	-15.32	-4.89	+13.34	-4.67	-2.76	+2.14	-2.66	-2.06	-0.50	-2.00	-2.37	
e. + Interleave Im-Txt	57.14	69.36	75.52	68.67	25.33	59.20	50.38	74.00	30.27	32.96	38.50	50.49	
$\Delta$ (vs. DirAns)	+0.00	-17.73	+1.40	+10.01	-4.67	-2.20	+1.78	+2.34	-2.13	+2.31	+0.50	-0.38	
f. + <i>Null-Tokens</i>	63.15	83.06	81.81	74.00	<b>32.00</b>	66.80	56.38	<b>77.66</b>	32.98	32.85	38.25	53.92	
$\Delta$ (vs. DirAns)	+6.01	-4.03	+7.69	+15.34	+2.00	+5.40	+7.78	+6.00	+0.58	+2.20	+0.25	+3.05	
g. + GRPO	<b>64.66</b>	83.87	81.81	<b>74.67</b>	30.66	<b>67.13</b>	<b>56.66</b>	77.00	<b>33.51</b>	<b>33.49</b>	38.50	<b>54.04</b>	
$\Delta$ (vs. DirAns)	+7.52	-3.22	+7.69	+16.01	+0.66	+5.73	+8.06	+5.34	+1.11	+2.84	+0.50	+3.17	

soning information in both the text and image modalities.

*SAT* [48] contains 175K simulated examples of spatial reasoning questions and answers with both single-image and multi-image inputs. We do not have any CoT reasoning trace data here. Hence, we primarily use this data during *stage 2 and 3* of the training process so that the model can free-form generalize the *Null-Tokens* towards the final answers for queries not primarily seen in the pre-training.

**Baselines.** All baselines are trained using the training datasets listed above. We explore four baseline approaches. **+DirAns** trains the base model directly on the final answer without any reasoning traces. We use the same data mix as our method. Details in appendix.

**+TextCoT** trains using the text-based reasoning traces from Video-R1 [17] and direct answers from ZebraCoT [30]. **+GRPO** further fine-tunes the above with GRPO [9, 17, 24] using only the direct answers from SAT [48] and some from Zebra-COT [30] and Video-R1 [17] to refine the reasoning traces. We use a group size of 2 due to memory constraints and following recent work [21] and a batch size of 256.

**+Interleave Im-Txt** replicates a recent approach [68] that uses latents to encode visual information and *retains* explicit, text-based reasoning traces. We follow a similar two-stage approach to our method. Instead of warming up the  $\langle \text{Null} \rangle$  with both image and text, we only use the image supervision as described in Section 3. Next, during stage 2, we relax the loss on the image  $\langle \text{Null} \rangle$  tokens. We interleave the  $\langle \text{Null} \rangle$  with explicit text and train with all the reasoning traces (substituting  $\langle \text{Null} \rangle$  for image thoughts when present) in our training datasets.

## 4.2. Main results

**Text-based reasoning improves base model, but hurts compared to direct answer fine-tuning.** We observe that supervising the model with text-based reasoning traces, while improves upon the base model performances as also found in concurrent work [17], *hurts* performance compared to directly tuning on the final answer of the same datasets. The results in Table 1 show that direct answer finetuning (row b) is a strong baseline, outperforming the text-based reasoning fine-tuning (row c) and also after GRPO optimization of the reasoning chains (row d). However, we do note that text-based reasoning tends to help on more reasoning-heavy splits compared to just fine-tuning with the final answer - BLINK Jigsaw and reasoning average (by  $\sim 2.1\%$ ) and VSI-Bench reasoning ( $\sim 0.4\%$ ).

**Interleaving image thoughts fail to improve significantly.** Recall, that the intuitive solution to “fix” text-based reasoning is to include visual thoughts (image latents) along with the explicit text thoughts [68]. The results for such an approach applied to our datasets (described in Section 4.1) are shown in Table 1 in row e. We see that it indeed performs better than text-based reasoning (row e vs d), with more gains seen on video reasoning splits (VSI reasoning) and on splits that require reasoning about action consequence and perspectives (SAT-Real and ERQA). However, it fails to improve overall from direct-answer finetuning across all benchmarks except SAT [48]. It also fails to improve on reasoning splits that are harder and out-of-domain such as BLINK IQ Tests. Empirically analyzing the interleaved reasoning outputs reveal two weaknesses - i) the model *rarely*

Table 2. Warming up *Null-Tokens* with multimodal image-text CoT (MM warm-up, row e) is crucial for performance, compared to no warm-up (row c), text-only warm up (row d). Data splits are described in Section 4.1.

Model	BLINK							SAT-R		VSI		ERQA	Avg(All)
	MV	RelDep	SpRel	Jig	IQT	Avg	Reas	Avg	Reas	Avg	Reas		
a. Qwen2.5-VL (7B)	39.00	61.29	<b>92.38</b>	58.66	25.33	55.33	41.00	59.00	23.96	22.96	<b>38.91</b>	44.30	
b. + DirAns FT	57.14	<b>87.09</b>	74.12	58.66	30.00	61.40	48.60	71.66	32.40	30.65	38.00	50.87	
c. + No warm-up	55.63	79.03	81.11	51.33	28.66	59.15	45.21	67.33	29.77	27.38	37.75	48.50	
$\Delta$ (vs. DirAns)	-1.51	-8.06	+6.99	-7.33	-1.34	-2.25	-3.39	-4.33	-2.63	-3.27	-0.25	-2.37	
d. + Text warm-up	59.39	<b>85.48</b>	85.31	67.33	32.00	65.90	52.91	71.33	32.02	<b>33.47</b>	38.50	51.94	
$\Delta$ (vs. DirAns)	+2.25	-1.61	+11.19	+8.67	+2.00	+4.50	+4.31	-0.33	-0.38	+2.82	+0.50	+1.07	
e. + MM warm-up	<b>63.15</b>	83.06	81.81	<b>74.00</b>	<b>32.00</b>	<b>66.80</b>	<b>56.38</b>	<b>77.66</b>	<b>32.98</b>	32.85	38.25	<b>53.92</b>	
$\Delta$ (vs. DirAns)	+6.01	-4.03	+7.69	+15.34	+2.00	+5.40	+7.78	+5.99	+0.58	+2.20	+0.25	+3.05	

switches to image thoughts and resorts to mostly text reasoning, and ii) if we prompt the model to force it to switch to image thoughts (more details in the supplementary), it actually reduces performance - *e.g.* overall, performance went down by 3% when forced to reason with image thoughts compared to letting the model choose (row e). We observe that the text reasoning still suffers from drifting away from visual inputs even after a visual thought, or the model doesn't switch to visual thoughts at the optimal timing (examples in supplementary). This suggests that while interleaving image thoughts may be helpful sometimes, the model still cannot effectively use it to think towards an accurate answer.

**Using modality-agnostic *Null-Tokens* performs best overall.** As shown in Table 1 row f and g, we see that our *Null-Tokens*, which are agnostic to text or image modality, perform best overall, including reasoning splits that harder out-of-domain tasks. Our *Null-Tokens* (after stage 2) (row f) improves compared to direct-answer finetuning (row b), where various other reasoning approaches (row c, d, e, f) fail to. Notably, we have strong improvements in reasoning about camera movements, jigsaw puzzles and IQ tests (under BLINK column) that require reasoning with visual and symbolic modalities. Finally, we observe that latest advancements in RL, GRPO refinement, when applied to our *Null-Tokens* (row g) can further improve the reasoning-heavy splits in BLINK and VSI-Bench. Improvements to interleaved image-text reasoning (row e) suggest that effective thinking compute requires *Null-Tokens* to be *modality-agnostic* rather than restricted to vision.

### 4.3. Ablations

We further ablate what causes the performance gains. We explore whether the *Null-Tokens* utilize the multimodal information in its reasoning latents. The model could just

be taking advantage of a wider computational pathway of meaningless tokens instead.

**No Warm-up.** If the model were to simply use *Null-Tokens* as a wider computational pathway, we would see gains if we only fine-tuned according to Stage 2 (Section 3 with the new tokens (without any multimodal information imparted into them) as extra compute for the model to optimize to arrive at the final answer. Hence, we perform this ablation and perform only Stage 2 tuning using direct answers from our training datasets

**Text-only Warm-up.** To ablate whether multimodal - *i.e.* including images with the text - is necessary, or text alone is sufficient, we warm-up the *Null-Tokens* using *only* the text-based CoT traces from our training data, discarding any traces that include interleaved images. We still use the final answers from the image COT trace dataset to not let domain differences in the datasets affect the performance.

**Our final approach.** Our final *Null-Tokens* approach, warms up the tokens on all available interleaved image-and-text reasoning traces in stage 1 (denoted by **MM warm-up**) before performing stage 2 training without any constraints on our latent tokens and only using the final answers from all our training datasets.

**Continuous Embeddings vs Discrete Tokens** Recall that the choices of using latent *Null-Tokens* tokens in stage 2 of the training (Section 3 and during inference are to use continuous embeddings that are recurrently fed in for  $k$  steps [25], or use discrete  $\langle \text{Null} \rangle$  tokens [22]. For the continuous ablation, in stage 2, for each latent  $\text{MULL}_k$ , we feed in the previous  $\text{MULL}_{k-1}$  embedding output before the language head of the Qwen model - both during inference and training.

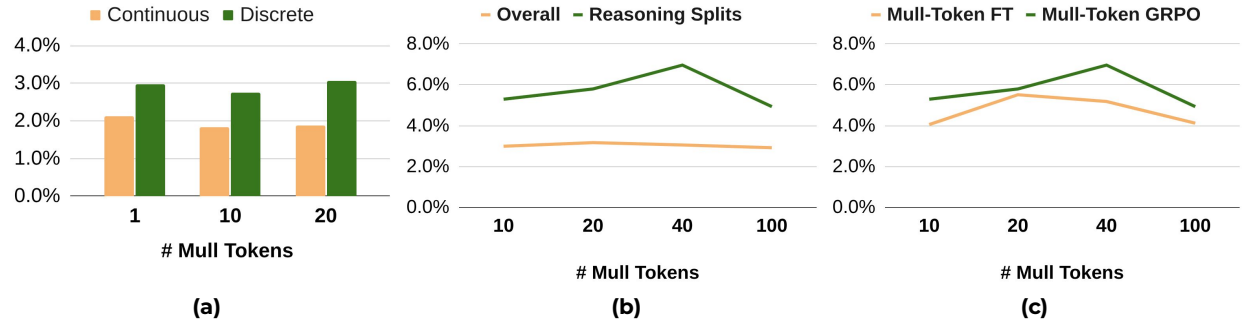


Figure 4. Hyperparameter choices in latent design. (a) Choice of continuous embeddings vs discrete tokens: We see that discrete performs better for each  $k$  (number of latent at test time) values. (b) The impact of number of latent tokens at test time: we see that too many latents can hurt performance. Reasoning splits tend to improve with more *Mull-Tokens*, but too many is still detrimental. (c) We see that performance scales with number of latent tokens more after GRPO since GRPO rewards the latent chain causally.

Table 3. We can add *Mull-Tokens* before predicting the explicit text reasoning and the final answer (row d). This improves answering performance compared to directly predicting the text reasoning (row b) or having interleaved visual thoughts with text reasoning (row c) before predicting the answer.

Model	BLINK	SAT-R	VSI	ERQA	Avg
a. Qwen 2.5 VL 7B	55.3	59.0	24.0	<b>38.9</b>	44.3
b. Text	58.0	68.3	30.5	38.8	48.9
c. Img + Text	59.2	<b>74.0</b>	30.3	38.5	50.5
d. <i>Mull-Tokens</i> + Text	<b>62.4</b>	72.0	<b>32.6</b>	37.3	<b>51.1</b>

#### 4.4. Analysis

***Mull-Tokens* with both image and text anchoring is crucial to performance.** While *Mull-Tokens* is effective, a question remains whether *Mull-Tokens* represents reasoning in a multimodal space or simply using a delay and extra compute [22] to improve performance. Hence, we ablate the choice of warming-up our *Mull-Tokens* as described in Section 4.3 and present the results in Table 2. We find that multimodal warm up allowing the *Mull-Tokens* to be multimodal - *i.e.* can hold meanings in either text or images - to be beneficial for performance. *Mull-Tokens* used simply as extra compute (row c) improves upon the base model by 4.2%, however, underperforms the direct answer baseline (row b) *Mull-Tokens* with text-only warm-up (row d) offers only a marginal 1.07% improvement over the direct answer fine-tuning baseline (row b), showing that a text-only warm-up, while somewhat beneficial, is still insufficient. Finally, warming up with both image and text achieves the highest gains (+3.05%) over the direct answer fine-tuning. This suggests that for *Mull-Tokens* to be effective, they *must* be pre-trained to handle *both* visual and textual information simultaneously.

**Discrete latent tokens over continuous embeddings.** Both strategies improve upon the direct answer finetuning

baseline as shown in Figure 4 - plot (a). However, discrete tokens perform better. Performance also starts to degrade with more continuous latents since errors accumulate with longer continuous embeddings, also seen by concurrent works [68]. Discrete also allows us to use the latest optimization tricks, such as token parallelism in standard frameworks for MLMs, resulting in significantly faster training and inference.

**The Effect of Number of Latent Tokens for Reasoning.** We investigate the effect of scaling the number of latent tokens used during inference - both after the *Mull-Tokens* FT and GRPO stages. Our model was trained using 20 latents. The results in Figure 4 - (b) and (c) show the trade-off. We first see that reasoning tasks tend to benefit more with higher number of tokens as shown in plot (b), but performance degrades with too many tokens- reminiscent of degradation due to overthinking in LLMs [62]. We see that performance scales more positively after the GRPO phase as shown in (c). We believe this might be because GRPO rewards the causal chain of tokens unlike SFT - *i.e.* during GRPO the chain of tokens need to lead to the correct answer, whereas during SFT, the model can memorize the final answer at the last latent step regardless of the chain.

**Adding *Mull-Tokens* can improve answering accuracy while also predicting the text rationale.** While *Mull-Tokens* without text-based reasoning improves overall performance, predicting the text-based reasoning (or rationale) can often be of educational and interpretable value. Hence, we explore if *Mull-Tokens* can also be appended before predicting both, the text rationale and the final answer. Intuitively, this allows the model to think in an abstract modality-agnostic space before verbalizing the rationale and predicting the answer. To perform this analysis, we include both the text rationale and the answers from the same training datasets in the Stage 2 (Section 3 of our training after the *Mull* tokens. Since we do not have reli-



**Q:** Given the first image with the lower right corner missing, can you tell which one of the second image or the third image is the missing part?



**Think:** <mull><mull><mull><mull> ...

- The [question] image has a crowd scene...
- The [first choice] image shows a close-up of what appears to be a person's hand holding something ... This image seems unrelated to the crowd scene.
- The [second choice] image features a woman in an orange outfit, also part of the crowd. **Her face and expression seem to align with the context of the crowd scene in the first image ...** [first choice] **doesn't seem to fit at all as it's too isolated and unrelated to the crowd scene.** [second choice] ... **shows a person who could be part of the crowd in the first image. Her expression and position make her seem like she could be continuing the scene.**

Oh, I see! The [second choice] provides a natural continuation of the crowd scene... <end\_think>

**Answer:** Choice B



**Q:** The camera is either moving clockwise (left) or counter-clockwise (right) around the object... Is the camera moving left or right when shooting the video?

**Think:** <mull><mull><mull><mull> ...  
<end\_think>

**Answer:** B. Moving right

Figure 5. *Mull*-Tokens tokens can be used in conjunction with text reasoning and the model can effectively decide when to also avoid using text reasoning depending on the task. For the example on the left, the model accurately uses *Mull*-Tokens along with some textual descriptive cues to reason about the missing piece. For the example on the right, the model decides to simply use the *Mull*-Tokens to directly predict the answer since textual descriptions are likely not helpful to detect camera motion.

able way to evaluate the rationales, we report the final answer accuracy in Table 3 and show some qualitative results in Figure 5. Interestingly, we note that the model decides to use text reasoning for certain tasks and just the *Mull*-Tokens tokens for tasks that may not need text reasoning to answer accurately. We observe that with *Mull*-Tokens, the answering accuracy after predicting the text rationale (row d) is higher than if we were to directly predict the rationale and answer (row b) or, if we were to simply use the interleaved image latents and text thoughts as in existing work [68] (row c).

## 5. Discussions

**Limitations.** Our experiments focused on the Qwen2.5-VL (7B) model [3]; while effective, the generalization of our findings to other backbones and model scales remains to be verified. A more intrinsic limitation of our approach is the lack of direct interpretability for the latent tokens. As these tokens are modality-agnostic—representing neither pure text nor pure image features—we cannot directly decode them into human-readable output. Our preliminary analysis mapping latents to their nearest vocabulary neighbors reveals that they are semantically consistent within task families (e.g., often mapping to "LetsCompare" for jigsaw tasks and "LetsThinkHmm" for more basic spatial relation tasks), but vary across different domains. However, without a method to decode these representations precisely, and a systematic evaluation protocol, the internal reasoning process remains partially opaque. However, we would like to emphasize that the scope of our paper is not to output more interpretable reasoning chains, but to analyze what serves as efficient thinking compute from a final answer performance

angle. We observe that a few *Mull*-Tokens readily improves performance over verbose, albeit interpretable, text thoughts.

**Future work.** We identify several key avenues for future work. First, extention of our approach to include diverse modalities such as 3D point clouds, audio, and other structured data, a direction currently constrained by the scarcity of suitable reasoning datasets. Finally, we see significant potential in integrating learning from world models [4] to discover robust causal reasoning chains, which is essential for bridging the remaining performance gap between current models and human capabilities.

**Conclusion.** In this work, we presented a novel fine-tuning paradigm that significantly improves visual reasoning capabilities compared to existing text-only or image-text interleaved approaches. We demonstrate that our multimodal latent <*Mull*> tokens provide a superior mechanism for reasoning: they are computationally more efficient, requiring significantly fewer tokens than verbose chain-of-thought methods, while simultaneously delivering higher accuracy. We hope this work paves the way for the exploration of efficient, high-performance reasoning techniques in the next generation of multimodal systems.

## Acknowledgments

We wish to thank Howard Zhou, Andre Araujo, Ye Xia and Alireza Fathi for helpful initial discussions, and Ellis Brown, Saining Xie, Romy Luo for their thoughts and feedback that helped polish the paper. We would like to thank the XCloud and Google Cloud Storage teams at Google, and Huggingface for providing a solid infrastructure to train and evaluate models.

## References

[1] Jinze Bai, Shuai Bai, Shusheng Yang, Shijie Wang, Sinan Tan, Peng Wang, Junyang Lin, Chang Zhou, and Jingren Zhou. Qwen-vl: A versatile vision-language model for understanding, localization, text reading, and beyond. *arXiv preprint arXiv:2308.12966*, 2023. 2, 3, 14

[2] Shuai Bai, Yuxuan Cai, Ruizhe Chen, Keqin Chen, Xionghui Chen, Zesen Cheng, Lianghao Deng, Wei Ding, Chang Gao, Chunjiang Ge, Wenbin Ge, Zhifang Guo, Qidong Huang, Jie Huang, Fei Huang, Binyuan Hui, Shutong Jiang, Zhao-hai Li, Mingsheng Li, Mei Li, Kaixin Li, Zicheng Lin, Junyang Lin, Xuejing Liu, Jiawei Liu, Chenglong Liu, Yang Liu, Dayiheng Liu, Shixuan Liu, Dunjie Lu, Ruilin Luo, Chenxu Lv, Rui Men, Lingchen Meng, Xuancheng Ren, Xingzhang Ren, Sibo Song, Yuchong Sun, Jun Tang, Jianhong Tu, Jian-qiang Wan, Peng Wang, Pengfei Wang, Qiyue Wang, Yuxuan Wang, Tianbao Xie, Yiheng Xu, Haiyang Xu, Jin Xu, Zhibo Yang, Mingkun Yang, Jianxin Yang, An Yang, Bowen Yu, Fei Zhang, Hang Zhang, Xi Zhang, Bo Zheng, Humen Zhong, Jingren Zhou, Fan Zhou, Jing Zhou, Yuanzhi Zhu, and Ke Zhu. Qwen3-vl technical report. *arXiv preprint arXiv:2511.21631*, 2025. 1

[3] Shuai Bai, Keqin Chen, Xuejing Liu, Jialin Wang, Wenbin Ge, Sibo Song, Kai Dang, Peng Wang, Shijie Wang, Jun Tang, et al. Qwen2.5-VL technical report. *arXiv preprint arXiv:2502.13923*, 2025. 2, 3, 5, 9

[4] Philip J. Ball and Jakob Bauer et al. Genie 3: A new frontier for world models, 2025. 9

[5] Mahtab Bigverdi, Zelun Luo, Cheng-Yu Hsieh, Ethan Shen, Dongping Chen, Linda G Shapiro, and Ranjay Krishna. Perception tokens enhance visual reasoning in multimodal language models. In *Proceedings of the Computer Vision and Pattern Recognition Conference*, pages 3836–3845, 2025. 1, 2, 3, 4

[6] Ellis Brown, Arijit Ray, Ranjay Krishna, Ross Girshick, Rob Fergus, and Saining Xie. SIMS-V: Simulated instruction-tuning for spatial video understanding, 2025. 1, 3

[7] Zikui Cai, Andrew Wang, Anirudh Satheesh, Ankit Nakhawa, Hyunwoo Jae, Keenan Powell, Minghui Liu, Neel Jay, Sungbin Oh, Xiyao Wang, et al. Morse-500: A programmatically controllable video benchmark to stress-test multimodal reasoning. *arXiv preprint arXiv:2506.05523*, 2025. 1

[8] Juhai Chen, Zhiyang Xu, Xichen Pan, Yushi Hu, Can Qin, Tom Goldstein, Lifu Huang, Tianyi Zhou, Saining Xie, Silvio Savarese, et al. Blip3-o: A family of fully open unified multimodal models-architecture, training and dataset. *arXiv preprint arXiv:2505.09568*, 2025. 1

[9] Liang Chen, Lei Li, Haozhe Zhao, Yifan Song, and Vinci. R1-v: Reinforcing super generalization ability in vision-language models with less than \$3. <https://github.com/Deep-Agent/R1-v>, 2025. Accessed: 2025-02-02. 4, 6

[10] Qiguang Chen, Libo Qin, Jinhao Liu, Dengyun Peng, Jian-nan Guan, Peng Wang, Mengkang Hu, Yuhang Zhou, Te Gao, and Wanxiang Che. Towards reasoning era: A survey of long chain-of-thought for reasoning large language models, 2025. 2

[11] Zhangquan Chen, Manyuan Zhang, Xinlei Yu, Xufang Luo, Mingze Sun, Zihao Pan, Yan Feng, Peng Pei, Xunliang Cai, and Ruqi Huang. Think with 3d: Geometric imagination grounded spatial reasoning from limited views. *arXiv preprint arXiv:2510.18632*, 2025. 2

[12] An-Chieh Cheng, Hongxu Yin, Yang Fu, Qiushan Guo, Ruihan Yang, Jan Kautz, Xiaolong Wang, and Sifei Liu. Spatial-rgrpt: Grounded spatial reasoning in vision-language models. In *Advances in Neural Information Processing Systems*, pages 135062–135093. Curran Associates, Inc., 2024. 2, 3

[13] Ethan Chern, Jiadi Su, Yan Ma, and Pengfei Liu. Anole: An open, autoregressive, native large multimodal models for interleaved image-text generation. *arXiv preprint arXiv:2407.06135*, 2024. 1

[14] Ethan Chern, Zhulin Hu, Steffi Chern, Siqi Kou, Jiadi Su, Yan Ma, Zhijie Deng, and Pengfei Liu. Thinking with generated images. *arXiv preprint arXiv:2505.22525*, 2025. 2

[15] Erik Daxberger, Nina Wenzel, David Griffiths, Haiming Gang, Justin Lazarow, Gefen Kohavi, Kai Kang, Marcin Eichner, Yinfai Yang, Afshin Dehghan, and Peter Grasch. Mm-spatial: Exploring 3d spatial understanding in multimodal LLMs, 2025. 3

[16] Guhao Feng, Bohang Zhang, Yuntian Gu, Haotian Ye, Di He, and Liwei Wang. Towards revealing the mystery behind chain of thought: A theoretical perspective. In *Advances in Neural Information Processing Systems*, pages 70757–70798. Curran Associates, Inc., 2023. 2

[17] Kaituo Feng, Kaixiong Gong, Bohao Li, Zonghao Guo, Yibing Wang, Tianshuo Peng, Benyou Wang, and Xiangyu Yue. Video-R1: Reinforcing video reasoning in MLLMs. *arXiv preprint arXiv:2503.21776*, 2025. 2, 4, 5, 6, 13

[18] Stephanie Fu, Tyler Bonnen, Devin Guillory, and Trevor Darrell. Hidden in plain sight: Vlms overlook their visual representations. *arXiv preprint arXiv:2506.08008*, 2025. 2

[19] Xingyu Fu, Yushi Hu, Bangzheng Li, Yu Feng, Haoyu Wang, Xudong Lin, Dan Roth, Noah A Smith, Wei-Chiu Ma, and Ranjay Krishna. BLINK: Multimodal large language models can see but not perceive. In *European Conference on Computer Vision*, pages 148–166. Springer, 2024. 2, 5

[20] Jonas Geiping, Sean McLeish, Neel Jain, John Kirchenbauer, Siddharth Singh, Brian R Bartoldson, Bhavya Kailkhura, Abhinav Bhatole, and Tom Goldstein. Scaling up test-time compute with latent reasoning: A recurrent depth approach. *arXiv preprint arXiv:2502.05171*, 2025. 3

[21] Scott Geng, Hamish Ivison, Chun-Liang Li, Maarten Sap, Jerry Li, Ranjay Krishna, and Pang Wei Koh. The delta learning hypothesis: Preference tuning on weak data can yield strong gains, 2025. 6

[22] Sachin Goyal, Ziwei Ji, Ankit Singh Rawat, Aditya Menon, Sanjiv Kumar, and Vaishnavh Nagarajan. Think before you speak: Training language models with pause tokens. In *International Conference on Learning Representations (ICLR)*, 2024. 2, 3, 4, 5, 7, 8

[23] Jiawei Gu, Yunzhuo Hao, Huichen Will Wang, Linjie Li, Michael Qizhe Shieh, Yejin Choi, Ranjay Krishna, and Yu

Cheng. Thinkmorph: Emergent properties in multimodal interleaved chain-of-thought reasoning. *arXiv preprint arXiv:2510.27492*, 2025. 1, 2, 3

[24] Daya Guo, Dejian Yang, Haowei Zhang, Junxiao Song, Peiyi Wang, Qihao Zhu, Runxin Xu, Ruoyu Zhang, Shirong Ma, Xiao Bi, et al. Deepseek-R1 incentivizes reasoning in LLMs through reinforcement learning. *Nature*, 645(8081):633–638, 2025. 2, 4, 6

[25] Shibo Hao, Sainbayar Sukhbaatar, DiJia Su, Xian Li, Zhitong Hu, Jason Weston, and Yuandong Tian. Training large language models to reason in a continuous latent space. *arXiv preprint arXiv:2412.06769*, 2024. 3, 4, 5, 7

[26] Yushi Hu, Weijia Shi, Xingyu Fu, Dan Roth, Mari Ostendorf, Luke Zettlemoyer, Noah A Smith, and Ranjay Krishna. Visual sketchpad: Sketching as a visual chain of thought for multimodal language models. *arXiv preprint arXiv:2406.09403*, 2024. 1, 2, 3

[27] Fucai Ke, Joy Hsu, Zhixi Cai, Zixian Ma, Xin Zheng, Xindi Wu, Sukai Huang, Weiqing Wang, Pari Delir Haghghi, Gholamreza Haffari, et al. Explain before you answer: A survey on compositional visual reasoning. *arXiv preprint arXiv:2508.17298*, 2025. 2

[28] Michael Kleinman, Matthew Trager, Alessandro Achille, Wei Xia, and Stefano Soatto. e1: Learning adaptive control of reasoning effort. *arXiv preprint arXiv:2510.27042*, 2025. 3

[29] Jason Lee, Jiafei Duan, Haoquan Fang, Yuquan Deng, Shuo Liu, Boyang Li, Bohan Fang, Jieyu Zhang, Yi Ru Wang, Sangho Lee, et al. Molmoact: Action reasoning models that can reason in space. *arXiv preprint arXiv:2508.07917*, 2025. 1, 2

[30] Ang Li, Charles Wang, Deqing Fu, Kaiyu Yue, Zikui Cai, Wang Bill Zhu, Ollie Liu, Peng Guo, Willie Neiswanger, Furong Huang, et al. Zebra-cot: A dataset for interleaved vision language reasoning. *arXiv preprint arXiv:2507.16746*, 2025. 1, 2, 5, 6, 14

[31] Chengzu Li, Wenshan Wu, Huanyu Zhang, Yan Xia, Shaoguang Mao, Li Dong, Ivan Vulić, and Furu Wei. Imagine while reasoning in space: Multimodal visualization-of-thought. *arXiv preprint arXiv:2501.07542*, 2025. 2

[32] Linjie Li, Mahtab Bigverdi, Jiawei Gu, Zixian Ma, Yinu Yang, Ziang Li, Yejin Choi, and Ranjay Krishna. Unfolding spatial cognition: Evaluating multimodal models on visual simulations. *arXiv preprint arXiv:2506.04633*, 2025. 1

[33] Ming Li, Jike Zhong, Shitian Zhao, Yuxiang Lai, and Kaipeng Zhang. Think or not think: A study of explicit thinking in rule-based visual reinforcement fine-tuning. *arXiv preprint arXiv:2503.16188*, 2025. 2

[34] Wenyan Li, Raphael Tang, Chengzu Li, Caiqi Zhang, Ivan Vulić, and Anders Søgaard. Lost in embeddings: Information loss in vision-language models. *arXiv preprint arXiv:2509.11986*, 2025. 2

[35] Benlin Liu, Amita Kamath, Madeleine Grunde-McLaughlin, Winson Han, and Ranjay Krishna. Visual representations inside the language model. *arXiv preprint arXiv:2510.04819*, 2025. 2

[36] Disheng Liu, Tuo Liang, Zhe Hu, Jierui Peng, Yiren Lu, Yi Xu, Yun Fu, and Yu Yin. Deconstructing spatial intelligence in vision-language models, 2025. 2

[37] Haotian Liu, Chunyuan Li, Qingyang Wu, and Yong Jae Lee. Visual instruction tuning. In *Advances in Neural Information Processing Systems*, pages 34892–34916. Curran Associates, Inc., 2023. 2, 3

[38] Ryan Liu, Jiayi Geng, Addison J. Wu, Ilia Sucholutsky, Tania Lombrozo, and Thomas L. Griffiths. Mind your step (by step): Chain-of-thought can reduce performance on tasks where thinking makes humans worse, 2025. 1

[39] Yanzuo Lu, Xin Xia, Manlin Zhang, Huafeng Kuang, Jianbin Zheng, Yuxi Ren, and Xuefeng Xiao. Hyper-bagel: A unified acceleration framework for multimodal understanding and generation, 2025. 2

[40] Mi Luo, Zihui Xue, Alex Dimakis, and Kristen Grauman. When thinking drifts: Evidential grounding for robust video reasoning, 2025. 2, 3, 5, 13

[41] Zixian Ma, Jianguo Zhang, Zhiwei Liu, Jieyu Zhang, Juntao Tan, Manli Shu, Juan Carlos Niebles, Shelby Heinecke, Huan Wang, Caiming Xiong, Ranjay Krishna, and Silvio Savarese. Taco: Learning multi-modal action models with synthetic chains-of-thought-and-action, 2024. 1

[42] Hanspeter A Mallot. *From geometry to behavior: An introduction to spatial cognition*. MIT Press, 2024. 1

[43] Kevins-Kokitsi Maninis, Kaifeng Chen, Soham Ghosh, Arjun Karpur, Koert Chen, Ye Xia, Bingyi Cao, Daniel Salz, Guangxing Han, Jan Dlabal, Dan Gnanapragasam, Mojtaba Seyedhosseini, Howard Zhou, and Andre Araujo. Tips: Text-image pretraining with spatial awareness, 2025. 3

[44] OpenAI. Thinking with images. <https://openai.com/index/thinking-with-images/>, 2025. 1, 2

[45] Pooyan Rahmanzadehgeravi, Logan Bolton, Mohammad Reza Taesiri, and Anh Totti Nguyen. Vision language models are blind. In *Proceedings of the Asian Conference on Computer Vision (ACCV)*, pages 18–34, 2024. 2

[46] Jeff Rasley, Samyam Rajbhandari, Olatunji Ruwase, and Yuxiong He. Deepspeed: System optimizations enable training deep learning models with over 100 billion parameters. In *Proceedings of the 26th ACM SIGKDD International Conference on Knowledge Discovery & Data Mining*, page 3505–3506, New York, NY, USA, 2020. Association for Computing Machinery. 5, 13

[47] Arijit Ray, Filip Radenovic, Abhimanyu Dubey, Bryan A. Plummer, Ranjay Krishna, and Kate Saenko. Cola: A benchmark for compositional text-to-image retrieval, 2023. 2

[48] Arijit Ray, Jiafei Duan, Reuben Tan, Dina Bashkirova, Rose Hendrix, Kiana Ehsani, Aniruddha Kembhavi, Bryan A Plummer, Ranjay Krishna, Kuo-Hao Zeng, et al. Sat: Spatial aptitude training for multimodal language models. *arXiv preprint arXiv:2412.07755*, 2024. 1, 2, 3, 5, 6, 13

[49] Zhenyi Shen, Hanqi Yan, Linhai Zhang, Zhanghao Hu, Yali Du, and Yulan He. CODI: Compressing Chain-of-Thought into Continuous Space via Self-Distillation. *arXiv preprint arXiv:2502.21074*, 2025. 2, 3

[50] Charlie Snell, Jaehoon Lee, Kelvin Xu, and Aviral Kumar. Scaling LLM test-time compute optimally can be more

effective than scaling model parameters. *arXiv preprint arXiv:2408.03314*, 2024. 3

[51] Quan Sun, Qiying Yu, Yufeng Cui, Fan Zhang, Xiaosong Zhang, Yueze Wang, Hongcheng Gao, Jingjing Liu, Tiejun Huang, and Xinlong Wang. Emu: Generative pretraining in multimodality. In *The Twelfth International Conference on Learning Representations*, 2024. 2

[52] Renliang Sun, Wei Cheng, Dawei Li, Haifeng Chen, and Wei Wang. Stop when enough: Adaptive early-stopping for chain-of-thought reasoning. *arXiv preprint arXiv:2510.10103*, 2025. 2

[53] Chameleon Team. Chameleon: Mixed-modal early-fusion foundation models. *arXiv preprint arXiv:2405.09818*, 2024. 1, 2

[54] CVBench Team. Cvbench: A benchmark for cross-video multimodal reasoning, 2025. 2

[55] Gemini Robotics Team, Saminda Abeyruwan, Joshua Ainslie, Jean-Baptiste Alayrac, Montserrat Gonzalez Arenas, Travis Armstrong, Ashwin Balakrishna, Robert Baruch, Maria Bauza, Michiel Blokzijl, et al. Gemini robotics: Bringing ai into the physical world. *arXiv preprint arXiv:2503.20020*, 2025. 2, 5

[56] Shengbang Tong, Ellis Brown, Penghao Wu, Sanghyun Woo, Manoj Middepogu, Sai Charitha Akula, Jihan Yang, Shusheng Yang, Adithya Iyer, Xichen Pan, Ziteng Wang, Rob Fergus, Yann LeCun, and Saining Xie. Cambrian-1: A fully open, vision-centric exploration of multimodal LLMs, 2024. 2

[57] Barbara Tversky and Masaki Suwa. *Thinking with sketches*, pages 75–84. Oxford University Press, 2009. 1

[58] Marina Vasilyeva and Stella F Lourenco. Development of spatial cognition. *Wiley Interdisciplinary Reviews: Cognitive Science*, 3(3):349–362, 2012. 1

[59] Jiayu Wang, Yifei Ming, Zhenmei Shi, Vibhav Vineet, Xin Wang, Yixuan Li, and Neel Joshi. Is a picture worth a thousand words? delving into spatial reasoning for vision language models, 2024. 1

[60] Jason Wei, Xuezhi Wang, Dale Schuurmans, Maarten Bosma, brian ichter, Fei Xia, Ed Chi, Quoc V Le, and Denny Zhou. Chain-of-thought prompting elicits reasoning in large language models. In *Advances in Neural Information Processing Systems*, pages 24824–24837. Curran Associates, Inc., 2022. 2

[61] Jason Wei, Xuezhi Wang, Dale Schuurmans, Maarten Bosma, Fei Xia, Ed Chi, Quoc V Le, Denny Zhou, et al. Chain-of-thought prompting elicits reasoning in large language models. *Advances in neural information processing systems*, 35:24824–24837, 2022. 1

[62] Zihao Wei, Liang Pang, Jiahao Liu, Jingcheng Deng, Shicheng Xu, Zenghao Duan, Jingang Wang, Fei Sun, Xunliang Cai, Huawei Shen, and Xueqi Cheng. Stop spinning wheels: Mitigating LLM overthinking via mining patterns for early reasoning exit, 2025. 8

[63] Chengyue Wu, Xiaokang Chen, Zhiyu Wu, Yiyang Ma, Xingchao Liu, Zizheng Pan, Wen Liu, Zhenda Xie, Xingkai Yu, Chong Ruan, and Ping Luo. Janus: Decoupling visual encoding for unified multimodal understanding and generation. In *Proceedings of the IEEE/CVF Conference on Computer Vision and Pattern Recognition (CVPR)*, pages 12966–12977, 2025. 2

[64] Yecheng Wu, Zhuoyang Zhang, Junyu Chen, Haotian Tang, Dacheng Li, Yunhao Fang, Ligeng Zhu, Enze Xie, Hongxu Yin, Li Yi, et al. Vila-u: a unified foundation model integrating visual understanding and generation. *arXiv preprint arXiv:2409.04429*, 2024.

[65] Jinheng Xie, Zhenheng Yang, and Mike Zheng Shou. Show-o2: Improved native unified multimodal models. *arXiv preprint arXiv:2506.15564*, 2025. 2

[66] Jihan Yang, Shusheng Yang, Anjali W. Gupta, Rilyn Han, Li Fei-Fei, and Saining Xie. Thinking in space: How multimodal large language models see, remember, and recall spaces. In *Proceedings of the IEEE/CVF Conference on Computer Vision and Pattern Recognition (CVPR)*, pages 10632–10643, 2025. 1, 2, 3, 5

[67] Shusheng Yang, Jihan Yang, Pinzhi Huang, Ellis Brown, Zihao Yang, Yue Yu, Shengbang Tong, Zihan Zheng, Yifan Xu, Muhan Wang, Daohan Lu, Rob Fergus, Yann LeCun, Li Fei-Fei, and Saining Xie. Cambrian-s: Towards spatial super-sensing in video, 2025. 2, 3

[68] Zeyuan Yang, Xueyang Yu, Delin Chen, Maohao Shen, and Chuang Gan. Machine mental imagery: Empower multimodal reasoning with latent visual tokens, 2025. 1, 2, 3, 4, 5, 6, 8, 9, 13

[69] Zhenrui Yue, Bowen Jin, Huimin Zeng, Honglei Zhuang, Zhen Qin, Jinsung Yoon, Lanyu Shang, Jiawei Han, and Dong Wang. Hybrid latent reasoning via reinforcement learning. *arXiv preprint arXiv:2505.18454*, 2025. 2

[70] Chi Zhang, Haibo Qiu, Qiming Zhang, Zhixiong Zeng, Lin Ma, and Jing Zhang. Deepsketcher: Internalizing visual manipulation for multimodal reasoning. *arXiv preprint arXiv:2509.25866*, 2025. 2

[71] Kaichen Zhang, Bo Li, Peiyuan Zhang, Fanyi Pu, Joshua Adrian Cahyono, Kairui Hu, Shuai Liu, Yuanhan Zhang, Jingkang Yang, Chunyuan Li, and Ziwei Liu. Lmms-eval: Accelerating the development of large multimodal models, 2024. 5

[72] Xinjie Zhang, Jintao Guo, Shanshan Zhao, Minghao Fu, Lunhao Duan, Jiakui Hu, Yong Xien Chng, Guo-Hua Wang, Qing-Guo Chen, Zhao Xu, et al. Unified multimodal understanding and generation models: Advances, challenges, and opportunities. *arXiv preprint arXiv:2505.02567*, 2025. 2

[73] Zhuosheng Zhang, Aston Zhang, Mu Li, Hai Zhao, George Karypis, and Alex Smola. Multimodal chain-of-thought reasoning in language models. *Transactions on Machine Learning Research*, 2024. 2

[74] Qingqing Zhao, Yao Lu, Moo Jin Kim, Zipeng Fu, Zhuoyang Zhang, Yecheng Wu, Zhaoshuo Li, Qianli Ma, Song Han, Chelsea Finn, Ankur Handa, Tsung-Yi Lin, Gordon Wetzstein, Ming-Yu Liu, and Donglai Xiang. Cot-vla: Visual chain-of-thought reasoning for vision-language-action models. In *Proceedings of the IEEE/CVF Conference on Computer Vision and Pattern Recognition (CVPR)*, pages 1702–1713, 2025. 2

[75] Xu Zheng, Zihao Dongfang, Lutao Jiang, Boyuan Zheng, Yulong Guo, Zhenquan Zhang, Giuliano Albanese, Runyi

Yang, Mengjiao Ma, Zixin Zhang, et al. Multimodal spatial reasoning in the large model era: A survey and benchmarks. <https://arxiv.org/abs/2510.25760>, 2025. 2

[76] Chenyue Zhou, Mingxuan Wang, Yanbiao Ma, Chenxu Wu, Wanyi Chen, Zhe Qian, Xinyu Liu, Yiwei Zhang, Junhao Wang, Hengbo Xu, et al. From perception to cognition: A survey of vision-language interactive reasoning in multimodal large language models. *arXiv preprint arXiv:2509.25373*, 2025. 2

[77] Qiji Zhou, Ruochen Zhou, Zike Hu, Panzhong Lu, Siyang Gao, and Yue Zhang. Image-of-thought prompting for visual reasoning refinement in multimodal large language models. *arXiv preprint arXiv:2405.13872*, 2024. 1

[78] Rui-Jie Zhu, Zixuan Wang, Kai Hua, Tianyu Zhang, Ziniu Li, Haoran Que, Boyi Wei, Zixin Wen, Fan Yin, He Xing, et al. Scaling latent reasoning via looped language models. *arXiv preprint arXiv:2510.25741*, 2025. 3

## 6. Appendix

In this supplementary document, we include further ablations in the training design choices, more details, and more insights into the shortcomings of related existing work versus our approach using qualitative examples. Finally, we also provide some qualitative examples to demonstrate our insights.

### 6.1. Training Details

We train using Deepspeed [46] stage 2 on 8 H100 GPUs. For the fine-tuned versions, we use a batch size of 1. We use a max gradient norm of 5 and use float bf16 precision for all our experiments, with a learning rate of  $1e-6$ . We freeze the vision encoder since we see minimal differences with training the visual encoder in our early experiments. All other parts of the model are fully fine-tuned.

The GRPO variants are trained using Deepspeed stage 3 to accommodate the significant increase in memory requirements. For the GRPO we use a reference model which is a frozen version of the same model. We use a group size of 2 (we run out of memory with a higher group size). We use a gradient accumulation size of 32 with 8 GPUs (data parallel). We use a beta (weighing the KL divergence) of 0.04. These hyperparameters follow the standard settings in the Video-R1 codebase [17]. We do GRPO for 200 steps - hence, 50K iterations ( $200 \times 32 \times 8$ ).

**Data mix used for each stage.** For stage 1, our goal is to primarily pretrain the *Mull-Tokens* to hold intermediate reasoning information. Hence, we primarily use the Video-R1 and Zebra-COT datasets which include reasoning traces. Specifically, we use a mixture of 40% Video-R1, 40% Zebra-COT, and 20% SAT for 200K iterations. In Stage 2 and 3, we now want the model to optimize the reasoning chains to data primarily not seen in the pretraining SFT mixture. Hence, we use a higher proportion of SAT

and still include some pretraining data to prevent domain forgetting following [48]. Specifically, we use a mixture of 60% SAT, and 20% each from Video-R1 and Zebra-COT for another 200K iterations.

For the baselines, we maintain the number of iteration steps to ensure fair comparison. For DirAns FT baseline - we also first train for 192K iterations (24K steps with data parallel on 8 GPUs) on 40% Video-R1, 40% Zebra-COT, and 20% SAT and then on 60% SAT, and 20% each from Video-R1 and Zebra-COT for another 192K iterations. We also tried training all in one stage for longer using 60% SAT, and 20% each from Video-R1 and Zebra-COT for 384K iterations and found the former to be a stronger baseline. For the TextCOT baseline, we first train for 192K iterations on 40% Video-R1 with text reasoning traces, 40% Zebra-COT answers only, and 20% SAT and then do GRPO for 50K steps on 60% SAT, and 20% each from Video-R1 (answers only) and Zebra-COT (answers only). We also tried the baseline of only first training on the Video-R1 since it is the only dataset with text reasoning traces before doing GRPO. However, we found the base model trained first with the entire mix to be a stronger starting point (higher benchmark numbers) for the GRPO.

### Prompting Strategies & Evaluation Settings

To strictly evaluate the reasoning capabilities of different model configurations, we employ three distinct prompting strategies. The specific template chosen determines whether the model relies on explicit textual generation, latent computation, or direct pattern matching. Additionally, a task-specific constraint (e.g., *"Please provide only the single option letter"* or *"Please provide a numeric answer"*) is appended to all templates based on the question type.

#### 1. Text-Reasoning Baseline (Video-R1).

To reproduce text-based reasoning baselines, we utilize the template established in prior work [17, 40, 68].

```
{Question}
Please think about this question as
if you were a human pondering deeply.
Engage in an internal dialogue using
expressions such as 'let me think',
'wait', 'Hmm', 'oh, I see', 'let's break
it down', etc, or other natural language
thought expressions. It's encouraged to
include self-reflection or verification
in the reasoning process. Provide your
detailed reasoning between the <think>
</think> tags, and then give your final
answer between the <answer> </answer>
tags.
```

#### 2. Image-text interleaved and *Mull-Tokens* (Ours).

For models based on our proposed *Mull-Tokens*, we em-

Table 4. Performance with different prompt strategies interleaving image and text thoughts. Explicitly instructing the model to think with images hurts performance compared to letting the model choose.

Model	BLINK							SAT-R	VSI		ERQA	All Avg
	MV	RelDep	SpRel	Jigsaw	IQT	Avg	Reason		Avg	Reason		
Qwen 2.5 VL 7B	39.0	61.3	92.4	58.7	25.3	55.3	41.0	59.0	24.0	23.0	38.9	44.3
+ Img-Txt (free-form)	57.1	69.4	75.5	68.7	25.3	59.2	50.4	74.0	30.3	33.0	38.5	50.5
+ Img-Txt (force im thought)	49.6	73.4	73.4	69.3	24.7	58.1	47.9	65.0	27.2	30.7	39.0	47.3
+ <i>Mull</i> -Tokens (our)	63.1	83.1	81.8	74.0	32.0	66.8	56.4	77.7	33.0	32.9	38.2	53.9

ploy a similar template. Since we do not explicitly verbalize the thoughts, we avoid phrases that encourage expressions like “Hmm”, “Oh, I see” etc.

```
{Question}
Please think about this question
deeply. It's encouraged to include
self-reflection or verification in the
reasoning process. Provide your final
answer between the <answer> </answer>
tags.
```

For image-text interleaved thoughts, we use Zebra-CoT [30] dataset. Each image is first encoded by the Qwen-VL [1] encoder, then all tokens are average-pooled into a single image feature vector. While allocating more latents to each image can likely help at the cost of higher compute, we leave such an ablation to future work. We use a discrete token mapped to the image feature, rather than using continuous embeddings for two reasons. First, we observed a slight degradation in performance. Second, continuous embeddings are slower due to recurrence loops during inference and training. During training, we use an explicit token `<im start>` followed by the `<latent>` token. The output of the `<latent>` is supervised to be the image feature.

For the *Mull*-Tokens approach, we simply append  $k$  `<Mull>` after the question prompt, providing the model with additional tokens as a multimodal thinking scratchpad.

### 3. Direct Answering (SFT & Base Model).

Finally, to evaluate the base model (zero-shot) and the standard Supervised Fine-Tuning (SFT) baseline, we use a *Direct* template. This is the most barebones setting to assess the model’s ability to map inputs directly to answers without intermediate computation steps.

```
{Question}
Provide your final answer between the
<answer> </answer> tags.
```

### Task-Specific Output Constraints.

To ensure the generated answers can be reliably parsed and evaluated against ground-truth, we append a format constraint to every prompt during evaluation. These con-

straints vary by task definition (e.g., Multiple Choice vs. Regression) and dictate the expected content within the `<answer>` tags. The specific suffixes used are:

- **Multiple Choice:** “Please provide only the single option letter (e.g., A, B, C, D, etc.) within the `<answer>` `</answer>` tags.”
- **Numerical / Regression:** “Please provide the numerical value (e.g., 42 or 3.14) within the `<answer>` `</answer>` tags.”
- **OCR:** “Please transcribe text from the image/video clearly and provide your text answer within the `<answer>` `</answer>` tags.”
- **Free-form:** “Please provide your text answer within the `<answer>` `</answer>` tags.”

### Fuzzy Logic Used to Extract Answers

To ensure robust evaluation, particularly when models produce verbose CoT outputs, we implement a fuzzy matching strategy to parse the final prediction as follows:

- **Pattern Extraction:** We first attempt to extract the answer by matching the prediction against a prioritized list of regular expression patterns. These include standard conversational markers and our enforced XML tags:
  - `r"<answer>\s*(.*?)\s*</answer>"`
  - `r"(?:the answer is|the
 correct answer is|final
 answer:)\s+([a-zA-Z0-9]+)"`
  - `r"I counted a total of\s+([\d+])"`
  - `r"count is\s+([\d+])"`
- **Validation & Numerical Extraction:** If a match is found, we check if the extracted content is a valid multiple-choice option (single letter A–Z). If the extracted text is not a letter, we attempt to parse it as a numerical value (integer or float) for regression or counting tasks.
- **Fallback Strategy:** In cases where the extraction fails or yields no numerical/categorical value, we perform a final fallback search for the last isolated capital letter (e.g., `r"\b[A-Z]\b"`) appearing in the raw text, assuming it

represents the final selection.

Empirically, we observe that the models usually adhere to the formatting instructions, with the vast majority of valid answers being successfully parsed directly from the `<answer>` tags via the first pattern.

## 6.2. Further Analysis and Ablations

In this section, we examine the shortcomings of modality switching, contrasting the inductive biases of interleaved image-text generation against our proposed joint reasoning approach. We identify specific issues, including ungrounded modality transitions and suboptimal scheduling, which hinder the performance of explicit switching baselines. Finally, we offer a preliminary analysis of the latent dynamics within our *Mull-Tokens*.

### The failure points with interleaving image-text

To investigate the feasibility of explicit modality switching for visual reasoning, we conducted a pilot study using a baseline model trained to interleave textual reasoning traces with discrete image latent tokens. We hypothesize that distinct processing steps for visual and textual thinking should allow for better interpretability and performance. However, our experiments reveal critical limitations in this paradigm.

**Bias Towards Textual Reasoning.** We observed a strong inductive bias in the model to rely solely on textual reasoning. When trained simply to solve problems, the model rarely invoked image latents at test time, preferring to reason exclusively via text. To address this, we introduced specific system prompts during training: one explicitly instructing the model to “think only using text” when the dataset included text-based reasoning traces and another to “think using both text and images” for the image-text interleaved training data.

Now, at test-time, we tried two approaches - one where we let the model decide by simply including the question without instructions for how to reason, and one where we append “think using both text and images” after the question to *force* the model to think using images. The results are shown in Table 4.

We observe two issues during inference:

- **Bias towards text-only reasoning:** When given the autonomy to choose its reasoning modality (i.e., without a forcing prompt), the model mostly reverts to text-only reasoning, and rarely switches to image latent thinking.
- **Forcing image thoughts degrades performance:** When we explicitly forced the utilization of image latents via the prompt, we observed a degradation in downstream task performance compared to the text-only baseline.

Table 4 presents the quantitative performance across multiple benchmarks, comparing our proposed approach against baseline configurations. Consistent with our qualitative findings, we observe that explicitly enforcing modality switching entails a performance trade-off.

### Performance Degradation with Forcing image

**Thoughts.** Comparing the *Img-Txt (free-form)* baseline with the *Img-Txt (force in thought)* setting reveals that prompting the model to use image thoughts leads to a reduction in overall performance. The average score across all benchmarks drops from 50.5% to 47.3%. Despite the aggregate decline, the forced image thought setting yields marginal but distinct improvements on specific tasks that inherently require visual simulation or geometric imagination- such as Jigsaw (68.7 → 69.3) and Relative Depth (RelDep) (69 → 73) - tasks that may require mentally manipulating visual patches to solve spatial puzzles, or visualizing depth maps or 3D structures from the 2D RGB inputs. However, while specific cases may benefit, we see an overall decline in performance compared to letting the model decide. These results suggest that while explicit image thoughts intuitively should contain valuable signals, the mechanism of explicit switching may be too brittle for general reasoning.

**Qualitative Analysis of Switching Failures.** To investigate performance degradation during explicit switching, we also qualitatively analyzed the model’s generated traces. We identified two prominent patterns in the failure cases that we show in Figure 6:

1. **Ungrounded Modality Transitions:** As shown in the top row of Figure 6, even when the model successfully generates an image latent (intended to process visual cues like fitting in the puzzle piece), the subsequent textual reasoning is often not properly grounded in that latent. In this example, The model correctly identifies that it needs to analyze the image choice’s edges and hence switches to the image thoughts. However, the text following it is incorrect. This suggests that the image latent did not contain enough information for the text thought to be properly grounded.
2. **Suboptimal Switching Scheduling:** The bottom row of Figure 6 demonstrates that the model struggles to identify the optimal moment to switch modalities. In this example, the model should have switched to latent after identifying the need to examine the options.

These findings suggest that rigid, explicit switching between modalities may be difficult and require more data. This limitation motivates our proposed approach: *modality-agnostic thinking tokens* that can jointly reason in a continuous space without explicit switching.

This motivates our modality agnostic *Mull-Tokens*. *Mull-Tokens* offers a simpler alternative where we do not need to switch between modalities, but rather think using latents trained to hold both visual and textual information jointly. Our proposed *Mull-Tokens* approach achieves the highest performance overall (Avg 53.9%). We posit that by enabling joint reasoning in a shared space, *Mull-Tokens* capture the benefits of visual imagination (e.g.,

high performance on RelDep and Jigsaw) without suffering the grounding losses associated with explicit modality switching. However, more interpretability studies will need to be done as future work to rigorously validate the function of *Null*-Tokens.

### **A preliminary attempt to interpret latents**

While our primary focus has been on performance, analyzing the semantic content of the *<Null>* latents presents a compelling avenue for future work. We conducted a preliminary analysis of the Euclidean distance between subsequent latents to see if latents encode different meanings. For *Null*-Tokens without a warm-up of image-text traces, the Euclidean distance between latents tapers off after a few steps before it converges, suggesting they become similar and add no new information. Our image-text warmed up latents maintains distances between steps. This indicates that the model avoids representational collapse and that each latent continues to contribute information (albeit useful or not). However, more analysis needs to be done by decoding or mapping the latents to actual reasoning images and closely controlled counterfactual images to understand and interpret the “meaning” of the *Null*-Tokens. With the absence of such data, we leave this analysis to future work. Our focus in the paper is to provide a more accurate, simple, and fast alternative to text reasoning or explicit image thoughts that require 100’s of tokens as reasoning before arriving at the answer.

## Text is not grounded after switching to image latent



[Jigsaw puzzle: Which option fits the black patch?  
GT Correct Ans: A

A B

THOUGHT 0: The problem asks to determine which of the second or third image is most suitable to fill the missing lower right corner of the first image. To decide, let's examine the content and edges of all three images.



THOUGHT 1: The first image is incomplete in the bottom right, indicated by a black box. We need to find the other two images' parts that could logically fit there. Let's analyze the second image's edges.



<IMLATENT>

*This text following the image latent is not correct.*

THOUGHT 2: The second image appears to show a continuation of the scene with signs and people, but its bottom edge does not align with the missing area in the first image. Let's look at the third image instead.



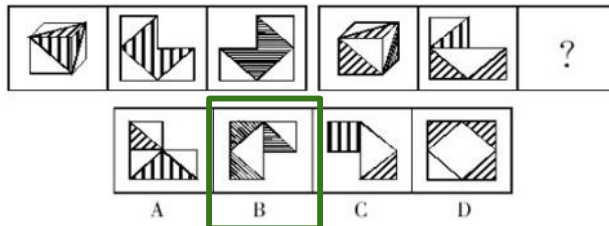
<IMLATENT>

THOUGHT 3: The third image shows a close-up of a sign and part of a person, including an arm and hand. Comparing its edges to the missing part in the first image, it seems like this section could seamlessly fit into the gap, as it contains elements (the arm, hand, and sign) that are also present in the larger scene of the first image.



...  
<answer>B</answer>

## Incorrect time of switching to image latents



[IQ Test: Which option fits the "?" ?]  
GT Correct Ans: B

...  
THOUGHT 1: Let's break down the pattern in the first sequence. Comparing the first two images, the shaded triangle moves position. The third image shows a rotation or flip of the triangle compared to the second. This suggests a sequential transformation.

<IMLATENT>

THOUGHT 2: For the second sequence, the cube and the triangle it contains undergo a similar transformation. The triangle's position and orientation change systematically from the first to the second image, and presumably, the third image continues this pattern.

<IMLATENT>

THOUGHT 3: Based on the identified pattern, the missing image should show a cube with a triangle inside it, where the triangle is in a configuration that follows the rotation or flipping rule observed in the examples. **Let me examine the options.**

Should have switched to image latents here instead of before.  
Text reason is wrong after

THOUGHT 4: Option A shows a cube with a triangle that fits the expected pattern of transformation. The triangle's position and the cube's orientation align with the established sequence. Therefore, option A is the most likely correct choice. </think>

<answer>A</answer>

Figure 6. Some qualitative examples of failures we observe with trying the existing approach of using explicit switching between image and text thoughts, motivating the need for our modality-agnostic *Null-Tokens*. Upper half: the image thought may not be enough for the text following it to be accurately grounded. The model correctly identifies that it needs to think in the image latent, but the text after is inaccurate. With our *Null-Tokens*, the model can free-form decide how many latents to allocate to the image since it doesn't need to explicitly switch back to text. Bottom half: Sometimes, the model cannot correctly identify when to switch to image latents. It switches at suboptimal times and doesn't switch to image latent even after identifying it needs to now compare the visual options (green bolded text). Our modality-agnostic *Null-Tokens* removes the need to explicitly switch between modalities.